Journal of Applied Polymer Science

An Ionic Liquid-Based Polymer with π-Stacked Structure as All-Solid-State Electrolyte for Efficient Dye-Sensitized Solar Cells

Guiqiang Wang,[1] Shuping Zhuo,[1] Yuan Lin[2]

[1]College of Chemical Engineering, Shandong University of Technology, Zibo 255049, China

[2]Institute of Chemistry, Chinese Academy of Science, Beijing 100080, China

Correspondence to: G. Wang (E-mail: wgqiang123@163.com)

ABSTRACT: An ionic liquid based polymer, poly(1-ethyl-3-(acryloyloxy)hexylimidazolium iodide) (PEAI), was synthesized and employed as electrolyte to fabricate all-solid-state dye-sensitized solar cells. The photophysical properties of PEAI were studied by UV–vis absorption spectroscopy and photoluminescence spectroscopy. PEAI exhibited significant hypochromism and red shift in UV–vis absorption spectra and large Stokes shifts in photoluminescence spectra, indicating the formation of a novel π-stacked structure in which the imidazolium rings in the side chain were stacked. Without iodine in its preparation, DSC with PEAI electrolyte achieved a conversion efficiency of 5.29% under AM 1.5 simulated solar light irradiation (100 mW cm^{-2}). The side-chain imidazolium π-π stacking in PEAI played a key role in the holes transport from the photoanode to the counter electrode. Both the open-circuit voltage and short-circuit current density showed decreases with the increase in the content of iodine in PEAI electrolyte. © 2012 Wiley Periodicals, Inc. J. Appl. Polym. Sci. 000: 000–000, 2012

KEYWORDS: photophysics; interface; electrochemistry; π-stacked structure; dye-sensitized solar cells

Received 24 January 2012; accepted 13 April 2012; published online
DOI: 10.1002/app.37933

INTRODUCTION

Since the great breakthrough made by O'Regan and Grätzel, dye-sensitized solar cells (DSCs) have attracted much interest in scientific research and industrial applications due to their high conversion efficiency, low cost, and simple fabrication process.[1,2] In such a photovoltaic system, visible light is absorbed by the dye, while the porous semiconductor separates effectively the electrons that are injected into the conduction band from the photoexcited dyes. The oxidized dyes are regenerated by the suitable redox couples added to the electrolyte. The redox couples also need to be renewed at the counter electrode, making the photoelectrochemical cell regenerative. As one of the key component of DSCs, the electrolyte plays an important role in determining the conversion efficiency and the long-term stability of the cell. At present, the most-efficient DSCs are fabricated using organic liquid electrolyte, and the conversion efficiency of the cell has exceeded 11%.[3,4] However, several practical problems related to the presence of organic liquid electrolytes (such as the leakage and evaporation of the liquid) are considered as some of the critical reasons limiting the long-term stability and practical application of DSCs.[5,6] Full replacement of the liquid electrolyte by an all-solid-state medium seems to be an effective solution to these problems. Therefore, all-solid-state electrolytes, such as p-type inorganic semiconductor,[7–9] organic hole-transport materials[10,11] and solvent-free composite polymer electrolyte,[12–16] were employed to fabricate the DSCs with good stability. Among these all-solid-state electrolytes, composite polymer electrolytes have attracted more attention due to its low cost, great safety and simple fabrication in wide range of shapes.

It is well known that the iodine is an essential component of composite polymer electrolytes in a conventional all-solid-state DSCs. To add the appropriate amount of iodine into polymer electrolyte can increase their ionic conductivity by forming the high-efficiency charge exchange tunnels.[17,18] However, the iodine can act as an oxidizing agent, corroding most high-conductivity metals. This feature limits the durability of the DSCs exceeding a few square centimeters in areas, in which metallic fingers were employed to overcome the large ohmic losses in the conductive glass substrate.

Recently, a few of reports have been made on the quasi-solid-state DSCs without iodine in their preparation.[19–21] These iodine-free quasi-solid-state cells achieved the considerable conversion efficiency and showed an unfailing stability. Besides, Meng and coworkers reported an all-solid-state electrolyte

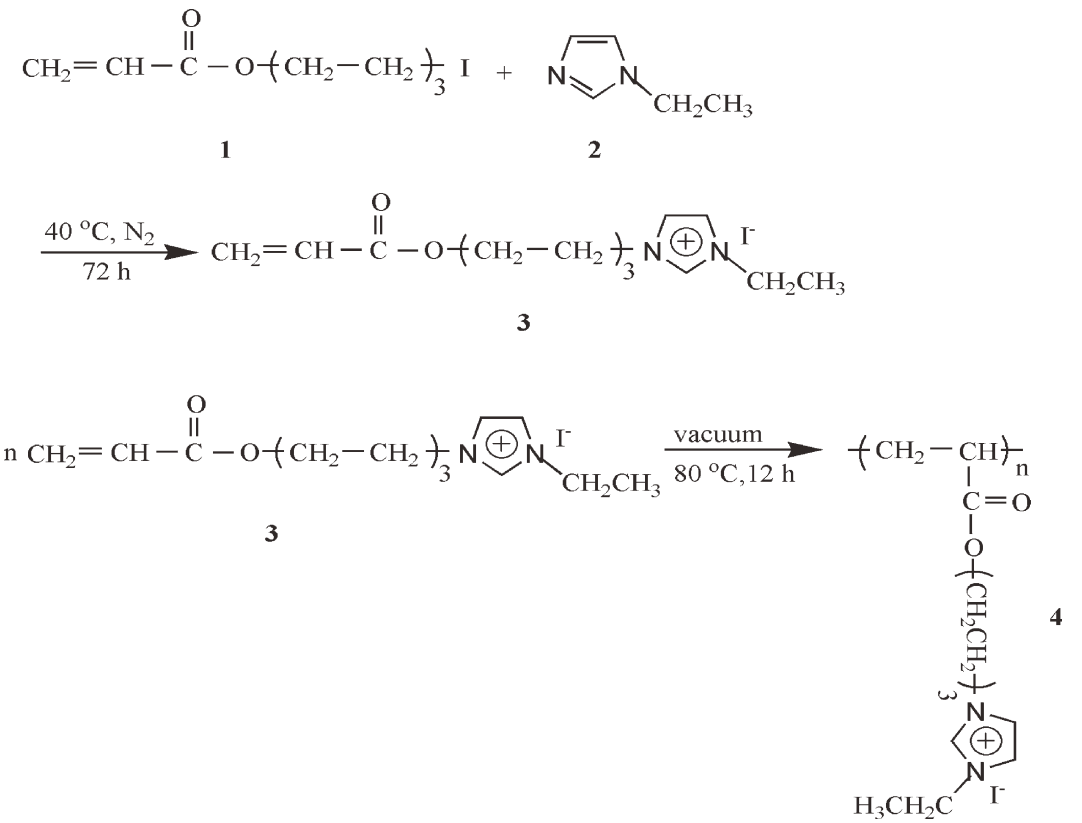

Scheme 1. Preparation processes of PEAI.

devoid of iodine based on LiI and 3-hydroxypropionitrile.[22] Using this electrolyte to fabricate DSC, a conversion efficiency of 5.4% was achieved under AM 1.5 simulated solar light illumination. In our recent work, an ionic liquid based polymer, poly(1-ethyl-3-(acryloyloxy)hexylimidazolium iodide) (PEAI), was synthesized and employed as the electrolyte to fabricate all-solid-state DSCs.[23] PEAI possesses the advantage of both ionic liquid and polymer, such as high conductivity and good stability. However, the properties and conductivity mechanism of the PEAI electrolyte was not fully understood at that time. In this article, the properties and the conductivity mechanism of PEAI electrolyte are further understood on the basis of UV–vis and photoluminescence spectra. We demonstrate that the side-chain imidazolium π-π stacking in PEAI electrolyte plays a key role in the holes transport from photoanode to counter electrode.

EXPERIMENTAL

Iodine and *N*-ethylimidazole (99%) were obtained from J & K Chemical. 1-iodohexyl-6-acrylate (95%) was purchased from Sigma-Aldrich, China, Diethyl ether (99.9%), acetonitrile (99.9%) and H_2PtCl_6 (99%) were obtained from Sinopharm Chemical Regent Beijing.

Synthesis processes of PEAI are shown in Scheme 1. Briefly, 1-iodohexyl-6-acrylate (1) was reacted with one and half molar amount of *N*-ethylimidazole (2) at 40°C for 72 h under nitrogen atmosphere. The product was purified by the extraction method with dehydrated diethyl ether to obtain pale yellow viscous liquid (1-ethyl-3-(acryloyloxy)hexylimidazolium iodide) (3). Obtained 1-ethyl-3-(acryloyloxy)hexylimidazolium iodide (EAI) were polymerized in bulk at 80°C under vacuum condition to obtain PEAI (4).

TiO_2 colloidal paste was prepared through hydrothermal method according to the literature.[24] The 5 wt % polystyrene particles with diameter of 40 nm were mixed with TiO_2 colloidal paste to increase the porosity of the TiO_2 film. The nanocrystalline TiO_2 film with the thickness of 5 μm was prepared by casting obtained TiO_2 colloidal paste onto fluorine-doped tin oxide (FTO) conducting glass and then sintering at 450°C for 30 min in air. Obtained TiO_2 electrodes were dipped into a 0.5 m*M* ethanol solution of N3 dye for 12 h at room temperature. Afterwards, the dye-sensitized electrodes were rinsed with ethanol and dried in the air. A platinized electrode prepared by the thermal decomposition of H_2PtCl_6 on the FTO glass substrate at 390°C was used as the counter electrode.

A PEAI solution was prepared by mixing 0.25 g PEAI and 10 mL acetonitrile under stirring. For the cell fabrication, PEAI solution was cast into dye-sensitized TiO_2 electrode and evaporated slowly. This same process was repeated for several times to ensure good filling of the pores in the TiO_2 electrode. Finally, a platinized electrode was pressed on the electrolyte. The fabricated cell was further dried in the vacuum oven for 48 h at 45°C to completely remove the residential solvent.

The UV–vis spectra were recorded on a Lambda 45 spectrophotometer. The photoluminescence spectra were obtained by using

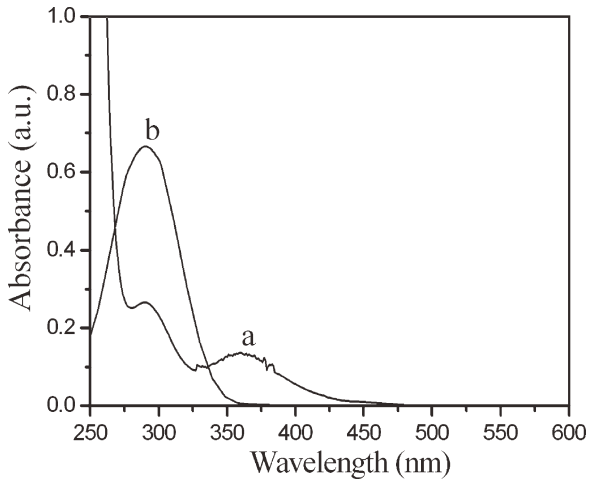

Figure 1. UV–vis absorption spectra of PEAI (a) and monomeric unite (i.e., EAI,) (b) in acetonitrile at room temperature. The solution concentration of PEAI and EAI is 1.13×10^{-5} *M* and 1.36×10^{-5} *M*, respectively.

LS-55 spectrophotometer (Perkin–Elmer). S-4300 model scanning electron microscopy (SEM, Hitachi Corp.) was used for the study of the interface between TiO_2 electrode and electrolyte. Ionic conductivity of solid-state electrolyte was measured by using HP 4192A impedance analyzer from 5 Hz to 13 MHz. The electrolyte was placed in a Teflon spacer ring, sandwiched with two stainless steel electrodes and sealed in a test cell. Photovoltaic performance of DSCs was measured on a M273 PAR potentiostat using a 500 W Xe lamp as a light source, the active area of the cell is 0.2 cm^2. Xe lamp was equipped with optical filter to give a simulated sun light at AM 1.5 (100 mW cm^{-2}). The incident light intensity was checked with a standard Si cell. Incident photon-to-current conversion efficiency (IPCE) was obtained using monochromatic irradiation from a Spectra-300i Triple Grating Monochromator with 400 W Xe lamp. A Solartron SI 1287 electrochemical interface equipped with a Solartron 1255B frequency response analyzer was used in the electrochemical impedance spectroscopy (EIS) measurements. The EIS measurements were carried out under illumination of 100 mW cm^{-2}.

RESULTS AND DISCUSSION

Photophysical Properties of PEAI

As shown in Scheme 1, PEAI is a comb polymer that imidazolium cations are fixed on the main chain by the flexible alkyl chain containing three ethylene units. Accordingly, only the iodide anion is mobile in PEAI. Benedetti et al. have reported that the cation trapping in the polymer electrolyte of DSCs resulted in the increase of transport number associated to iodide species, and then improved both the open-circuit voltage and the short-circuit current density of the cell.[25] Therefore, such a mono-ion transport feature is favorable as all-solid-state electrolyte to replace conventional organic liquid electrolyte used in DSCs. Because of the conjugation effect of imidazolium ring and the steric hindrance of polymer backbone, the attraction between the cation and the iodide anion is weak, resulting in easy diffusion of iodide anions in PEAI. Fast diffusion of iodide species in the electrolyte is of prime importance for a high regeneration rate of oxidized dye formed after electrons transfer.

The absorption and emission spectra of PEAI indicated characteristic profiles based on its structure. Figure 1 shows the UV–vis absorption spectrum of PEAI in acetonitrile at room temperature, along with that of the unstacked monomeric unit (EAI). The UV–vis absorption spectrum of PEAI indicates a significant hypochromism and has the broader red-shifted peaks compared with that of EAI, suggesting that the side-chain imidazolium rings in PEAI are stacked and the chromophore-to-chromophore distance is short enough to cause a π-π interaction in the ground state. The observed red shift of the absorption bands means that electronic interaction between neighboring imidazolium ring in the ground state lowered the excitation energy of PEAI. In main-chain conjugated polymers, a longer chain length results in a significantly reduced band gap.[26] Electronic interaction between closely stacked but not covalently bonded aromatic groups may also make the band gap narrower from present results as well as some other research works,[27] although the effect seems to be smaller as compared with that for main-chain conjugated polymers.

Figure 2 exhibits the emission spectra of PEAI and EAI in acetonitrile. The emission spectrum of PEAI indicated an emission bands around 575 nm, while that of EAI shows a short-wavelength emission bands around of 334 nm. The large stokes shift of PEAI (288 nm) relative to that of the unstacked EAI (42 nm) can be attributed to the delocalization of the excited energy over neighboring imidazolium ring along the polymer main chain, which indicates the formation of π-π stacking interaction among side-chain imidazolium ring. This is consistent with the result of UV–vis absorption spectra.

Conductivity of PEAI

The π-π stacked aromatic groups can provide the favorable channel for the charge transport.[28] Therefore, PEAI tend to

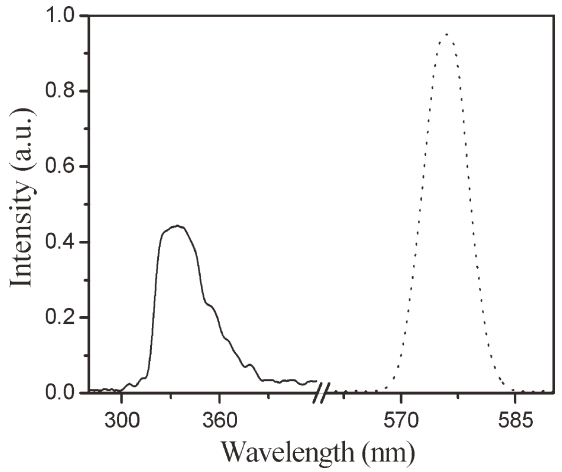

Figure 2. Emission spectra of PEAI (dot line) and EAI (solid line) in acetonitrile at room temperature. The excitation wavelength was 285 nm (EAI) and 288 nm (PEAI). The solution concentration of PEAI and EAI is 1.13×10^{-5} *M* and 1.36×10^{-5} *M*, respectively.

Applied Polymer SCIENCE

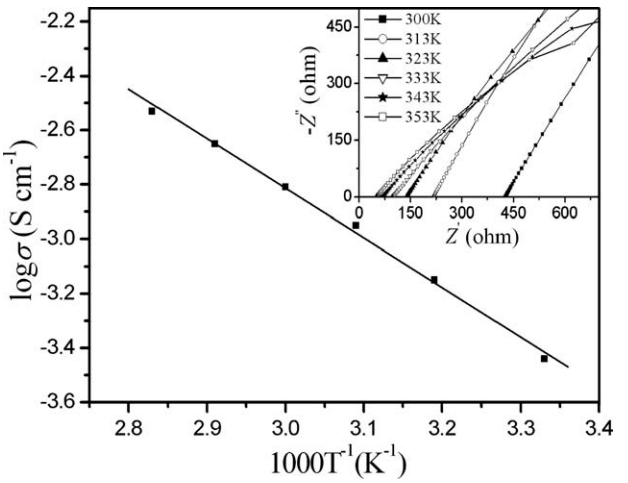

Figure 3. Temperature dependence of the conductivity for PEAI. The inset shows Nyquist plots for PEAI at different temperatures.

exhibit a good conductivity. The temperature dependence of the conductivity for PEAI is shown in Figure 3. The conductivities were obtained from impedance measurements, measured in sandwich cells composed of two stainless steel electrodes separated by a Teflon spacer ring and filed with PEAI electrolyte. The inset of Figure 3 shows the Nyquist plots for PEAI at different temperature. As can be seen from this figure, the conductivity is increasing when the temperature is increasing simultaneously in the observed temperature range, the relationship obeys the Arrhenius eq. (1):

$$\sigma = A \exp\left(\frac{-E_A}{k_B T}\right) \quad (1)$$

where σ is the conductivity, A is the pre-exponentional factor, E_A is the activation energy, k_B is the Boltzmann's constant. It suggests a thermal activation mechanism for the charge transport in PEAI. According to eq. (1), Arrhenius plot of conductivity vs. temperature in Figure 3 gives the activation energy for charge transport of 33.24 kJ mol^{-1}. At room temperature (25°C), PEAI exhibits a conductivity of 3.63×10^{-4} S cm^{-1}, which is comparable with the value reported for solid-state polymer electrolyte systems.[14,29]

Photovoltaic Performance

It is well known that a completed pore filling of dye-sensitized TiO_2 electrode and a good wetting of TiO_2 surface are crucial for an efficient all-solid-state DSC. We used PEAI as electrolyte to fabricate all-solid-state DSCs and examined the penetration of PEAI electrolyte in TiO_2 film by the cross-sectional SEM images of TiO_2 electrode. Figure 4 shows the cross-sectional SEM images of nanocrystalline TiO_2 electrodes before and after introducing PEAI electrolyte. Before introducing PEAI electrolyte, the TiO_2 nanoparticles and the pores between TiO_2 nanoparticles are distinguishable. After the electrolyte was added, the TiO_2 nanoparticles became indistinct and the pores disappeared. This indicates that the PEAI electrolyte cover the TiO_2 nanoparticles and penetrate into the pores of TiO_2 film, suggesting a good contact between TiO_2 nanoparticles and PEAI electrolyte throughout the TiO_2 layer. These features are favorable for the

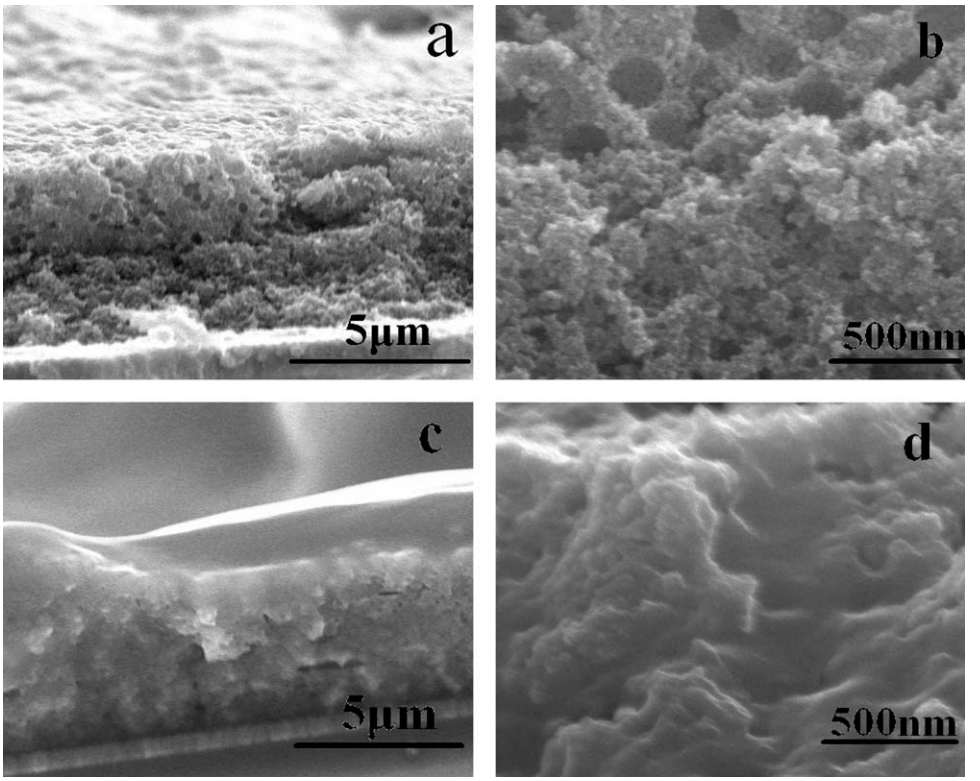

Figure 4. Cross-sectional SEM images for the interface of TiO_2 electrode with PEAI electrolyte, (a) and (b) before introducing PEAI electrolyte, (c) and (d) after introducing PEAI electrolyte.

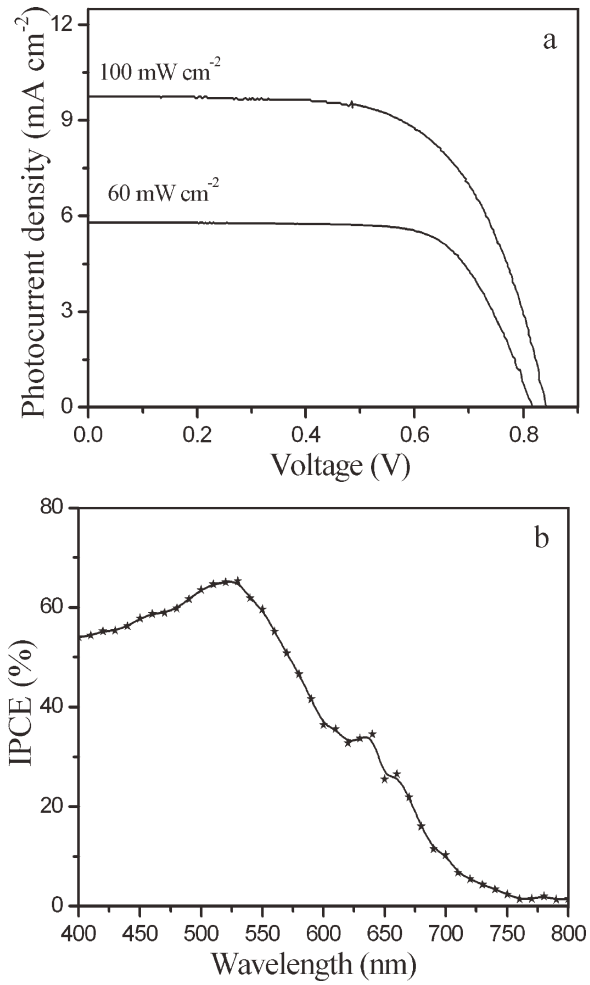

Figure 5. (a) Photocurrent density–voltage characteristics of DSC with PEAI electrolyte under illumination of 100 and 60 mW cm^{-2}, respectively; (b) Photocurrent action spectrum of DSC with PEAI electrolyte.

regeneration of oxidized dye molecules and reducing the recombination reaction between the conduction band electrons of TiO_2 and the oxidized dye molecules.

The photovoltaic performance of DSCs based on PEAI electrolyte was measured under AM 1.5 simulated solar light illumination. Figure 5(a) presents the photocurrent density–voltage curves of the cell under various light-intensity irradiations. At irradiation of 100 mW cm^{-2}, the open-circuit voltage (V_{oc}), the short-circuit current density (J_{sc}) and the fill factor (FF) of the DSC with PEAI electrolyte are 0.839 V, 9.75 mA cm^{-2} and 0.65, respectively, yielding an overall energy conversion efficiency (η) of 5.29%. The conversion efficiency is increased to 5.64% under illumination of 60 mW cm^{-2}. The photocurrent action spectrum of DSC with PEAI electrolyte is shown in Figure 5(b). The IPCE is defined as the number of electrons generated by light in the external circuit divided by the number of incident photons. The IPCE value of this device exceeds 55% in a broad spectral range from 430 to 560 nm, reaching its maximum of about 65% at 530 nm.

It should be pointed out that this all-solid-state electrolyte is composed of only one component (i.e., PEAI) and the cell in

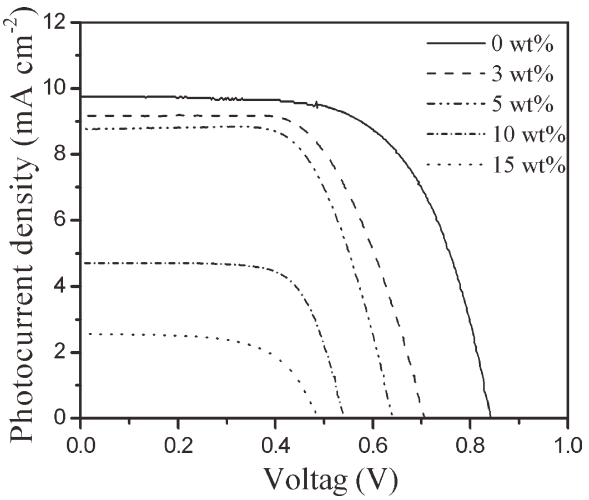

Figure 6. Photocurrent density–voltage characteristics of DSCs with PEAI electrolyte containing various iodine contents, measured under illumination of 100 mW cm^{-2}.

our study works at high efficiency without the addition of iodine to electrolyte. Although the iodine is an essential component of the electrolyte in a conventional DSC,[30] introducing the iodine into the PEAI electrolyte is not necessary and even detrimental in our case as can be seen from Figure 6. Figure 6 exhibits the comparison of photocurrent density–voltage curves for the standard iodine-free cell and iodine-added cells of various iodine contents. The photovoltaic parameters are summarized in Table I. Apparently, the cell works best with an iodine-free electrolyte, and the photovoltaic parameters of the cell decrease with the increase of iodine content in PEAI electrolyte. Decreased efficiency with increased iodine concentration also has been observed by Ikeda et al.[20] They found that incorporation of iodine as an initial component of electrolyte is not needed to drive their solid-state DSC and both of photovoltage and photocurrent is reduced by increased content of iodine.

Given the high concentration of iodide in PEAI electrolyte, increasing the content of iodine can increase the concentration of triiodide at the interface between TiO_2 films and electrolyte. It enhances the recombination of injected conduction band electrons with the triiodide as indicated in Figure 7(a). Figure 7(a) shows Nyquist plots of DSCs with PEAI electrolyte containing various iodine contents measured at open-circuit voltage under illumination. At open-circuit voltage and in sunlight, all the

Table I. Photovoltaic Parameters of DSC with PEAI Electrolyte Containing Various Iodine Contents

Iodine content (wt %)	V_{oc} (V)	J_{sc} (mA cm^{-2})	FF	η (%)
0	0.838	9.75	0.65	5.29
3	0.704	9.16	0.63	4.06
5	0.636	8.77	0.66	3.68
10	0.541	4.72	0.71	1.81
15	0.482	2.56	0.64	0.79

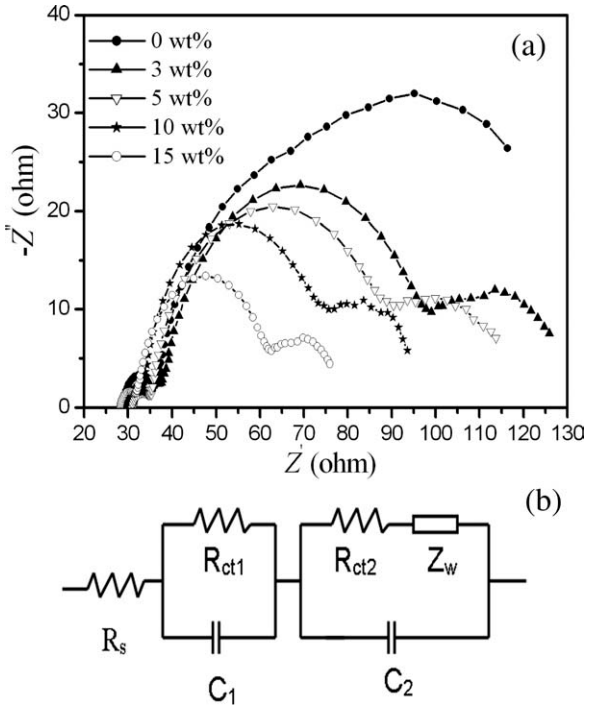

Figure 7. (a) Nyquist plots of DSCs with PEAI electrolyte containing various iodine contents, measured at 100 mW cm^{-2} light intensity under open-circuit voltage. (b) Equivalent circuit for the impedance spectra in (a).

injected electrons are recaptured by triiodide while oxidized dye is regenerated by iodide. Three typical semicircles in Nyquist plots shown in Figure 7(a) can be assigned to the charge transport in electrolyte, the electron recombination at the interface of TiO_2 film with electrolyte and the charge transfer process at counter electrode in the order of increasing frequency. The equivalent circuit of this model is shown in Figure 7(b). By fitting the plots in Figure 7(a) with *Z*-view software, the charge-transfer resistance on the counter electrode (R_{ct1}) and TiO_2 film (R_{ct2}) and the chemical capacitance (C_2) for the TiO_2/electrolyte interface are obtained and listed in Table II. As shown in Table II, R_{ct2} and C_2 decreases with the increase of the iodine content in electrolyte while R_{ct1} has almost no change. This indicates that electron recombination with triiodide is enhanced due to the augmentation of triiodide concentration. Furthermore, increasing content of iodine also leads to enhanced light absorption by the electrolyte existing in the porous dye-sensitized TiO_2 film, which decreases the light harvesting of dye molecules.[31] Therefore, both V_{oc} and J_{sc} show decrease with the increase in the content of iodine.

The photocurrent amplitude of DSCs with PEAI electrolyte is fairly stable under continuous illumination and during repeated measurements. This indicates that PEAI can provide sufficient iodide for the regeneration of the oxidized dye under illumination and the holes can be quickly and effectively transport from the photoanode to the counter electrode. In conventional DSCs, the holes are transported from the dye to the counter electrode mainly by the physical diffusion of triiodide and electron exchange reaction between iodide and triiodide.[32,33] Although it is deduced that a trace amount of triiodide is formed from

Table II. Impedance Parameters of DSCs with PEAI Electrolyte Containing Various Iodine Contents

Iodine content (wt %)	R_{ct1} (Ω cm^2)	R_{ct2} (Ω cm^2)	C_2 (μF)
0	0.8	15.5	167
3	0.8	7.5	154
5	0.6	6.5	139
10	0.5	4.5	131
15	0.5	3	126

PEAI at the dye/electrolyte interfacial region after irradiation in our case, it is too little to effectively transport the holes from the dye to the counter electrode. The absorption and emission features of PEAI shown in Figures 1 and 2 suggest that it possesses a novel π-stacked structure in which the imidazolium rings in the side chain are stacked. The π-stacked aromatic ring chain can favor the holes transport. This has been verified by the work of Nakano and coworkers.[28] Therefore, the π-stacked imidazolium ring chain in PEAI plays a key role in the holes transport from photoanode to counter electrode in our case.

CONCLUSIONS

PEAI was synthesized and successfully used as iodine-free electrolyte to fabricate all-solid-state DSCs. The absorption and emission features of PEAI indicated that it possesses a novel π-stacked structure in which the imidazolium rings in the side chain are stacked. PEAI exhibited a conductivity of 3.63×10^{-4} S cm^{-1} at room temperature. Without the addition of iodine, all-solid-state DSC with PEAI electrolyte achieved a conversion efficiency of 5.29% under simulated solar light illumination (AM 1.5, 100 mW cm^{-2}). The π-stacked structure in PEAI played a key role in the holes transport from photoanode to counter electrode. Incorporating iodine into PEAI electrolyte resulted in the decrease of both the short-circuit current density and the open-circuit voltage due to the light absorption by iodine and the enhancement of recombination of conduction band electrons with triiodide. This study may provide a means to design and prepare efficient novel electrolyte for all-solid-state DSCs with good stability.

ACKNOWLEDGMENTS

This work was supported by Shandong Provincial Natural Science Foundation (No. ZR2010BM038).

REFERENCES

1. O'Regan, B.; Grätzel, M. *Nature* **1991,** *353*, 737.
2. Grätzel M. *J. Photochem Photobiol. A Chem.* **2004,** *164*, 3.
3. Nazeeruddin, M. K.; Angelis, F. D.; Fantacci, S.; Selloni, A.; Viscardi, G.; Liska, P.; Ito, S.; Takeru, B.; Grätzel, M. *J. Am. Chem. Soc.* **2005,** *127*, 16835.
4. Yella, A.; Lee, H.; Tsao, H; Yi, C.; Chandiran, A. K.; Nazeeruddin, M. K.; Diau, E. W.; Yeh, C.; Zakeeruddin, S. M.; Grätzel, M. *Sicence* **2011,** *334*, 629.
5. Bai, Y.; Cao, Y.; Zhang, J.; Wang, M.; Li, R.; Wang, P.; Zakeeruddin, S. M.; Grätzel, M. *Nat. Mater.* **2008,** *7*, 626.

6. Kroeze, J. E.; Hirata, N.; Schmidt-Mende, L.; Orizu, C.; Ogier, S. D.; Carr, K.; Grätzel, M.; Durrant, J. R. *Adv. Funct. Mater.* **2006,** *16*, 1832.
7. O'Regan, B.; Lenzmann, F.; Muis, R.; Wienke, J. *Chem. Mater.* **2002,** *14*, 5023.
8. Konno, A.; Kitagawa, T.; Kida, H.; Kumara, G. R. A.; Tennakone, K. *Curr. Appl. Phys.* **2005,** *5*, 149.
9. Meng, Q.; Takahashi, K.; Zhang, X.; Sutanto, I.; Rao, T.; Sato, O.; Fujishima, A. *Langmuir* **2003,** *19*, 3572.
10. Snaith, H. J.; Moule, A. J.; Klein, C.; Meerholz, K.; Friend, R. H.; Grätzel, M. *Nano Lett.* **2007,** *7*, 3372.
11. Saito, Y.; Fukuri, N.; Senadeera, R.; Kitamura, T.; Wada, Y.; Yanagida, S. *Electrochem. Commun.* **2004,** *6*, 71.
12. Lan, Z.; Wu, J.; Lin, J.; Huang, M. *J. Appl. Polym. Sci.* **2010,** *116*, 1329.
13. Bandara, T. M. W. J.; Dissanayake, M. A. K. L.; Ileperuma, O. A.; Varapra Than, K.; Vignarooban, K.; Mellande, R. B. E. *J. Solid. State. Electrochem.* **2008,** *12*, 913.
14. Stergiopoulos, T.; Arabatzis, L. M.; Katsaros, G.; Falaras, P. *Nano Lett.* **2002,** *2*, 1259.
15. Han, H.; Liu, W.; Zhang, J.; Zhao, X. *Adv. Funct. Mater.* **2005,** *15*, 1940.
16. Nogueira, A. F.; Durrant, J. R.; De Paoli, M. A. *Adv. Mater.* **2001,** *13*, 826.
17. Wu, J.; Hao, S.; Lan, Z.; Lin, J.; Huang, M.; Huang, Y.; Li, P.; Yin, S.; Sato, T. *J. Am. Chem. Soc.* **2008,** *130*, 11568.
18. Shi, J.; Wang, L.; Liang, Y.; Peng, S.; Cheng, F.; Chen, J. *J. Phys. Chem. C* **2010,** *114*, 6814.
19. Lee, C.; Chen, P.; Vittal, R.; Ho, K. *J. Mater. Chem.* **2010,** *20*, 2356.
20. Ikeda, N.; Teshima, K.; Miyasaka, T. *Chem. Commun.* **2006,** *42*, 1733.
21. Lei, B.; Fang, W.; Hou, Y.; Liao, J.; Kuang, D.; Su, C. *J. Photochem. Photobiol. A Chem.* **2010,** *216*, 8.
22. Wang, H.; Li, H.; Xue, B.; Wang, Z.; Meng, Q.; Chen, L. *J. Am. Chem. Soc.* **2005,** *127*, 6394.
23. Wang, G.; Wang, L.; Zhuo, S.; Fang, S.; Lin, Y. *Chem. Commun.* **2011,** *47*, 2700.
24. Li, M.; Feng, S.; Fang, S.; Xiao, X.; Li, P.; Zhou, X.; Lin, Y. *Electrochim. Acta* **2007,** *52*, 4858.
25. Benedetti, J. E.; De Paoli, M. A.; Nogueira, A. F. *Chem. Commun.* **2008,** *44*, 1121.
26. Houk, K. N.; Lee, P. S.; Nendel, M, *J. Org. Chem.* **2001,** *65*, 5517.
27. Nakano, T.; Yade, T. *J. Am. Chem. Soc.* **2003,** *125*, 15474.
28. Coropceanu, Y.; Nakano, T.; Gruhn, N. E.; Kwon, O.; Yade, T.; Katsukawa, K.; Brédas, J. *J. Phys. Chem. B* **2006,** *110*, 9482.
29. Xiang, W.; Zhou, Y.; Yin, X.; Zhou, X.; Fang, S.; Lin, Y. *Electrochim. Acta* **2009,** *54*, 4186.
30. Hao, F.; Lin, H.; Zhang, J.; Zhuang, D.; Liu, Y.; Li, J. *Electrochim. Acta* **2010,** *55*, 7225.
31. Kubo, W.; Kambe, S.; Nakade, S.; Kitamura, T.; Hanabusa, K.; Wada, Y.; Yanagida, S. *J. Phys. Chem. B* **2003,** *107*, 4374.
32. Kawano, R.; Watanabe, M. *Chem. Commun.* **2003,** *39*, 330.
33. Hao, F.; Lin, H.; Zhang, J.; Li, J. *J. Power Source* **2011,** *196*, 1645.